communications in mathematical
match
and in computer chemistry

no. 44, October 2001

MATCDY (44) 65 - 92 (2001)

ISSN 0340 - 6253

THE EFFECTS OF RETINOIDS UPON EPITHELIAL DIFFERENTIATION OF HAMSTER TRACHEA, INDUCTION OF ORNITHINE DECARBOXYLASE AND PROMOTION OF TUMORS IN MOUSE EPIDERMIS. A QSAR STUDY BY MTD METHOD

Dan Ciubotariu,[a,e]* Adrian Grozav,[a] Valentin Gogonea,[b] Ciprian Ciubotariu,[c] Mihai Medeleanu,[d] Dan Dragoş,[a] Marian Pasere,[a] and Zeno Simon.[e]

[a] Department of Organic Chemistry, Faculty of Pharmacy, P-ta Eftimie Murgu No. 2 1900 Timisoara, ROMANIA

[b] Department of Chemistry, Cleveland State University, Science Building Room 422 2351 Euclid Avenue, Cleveland, Ohio 44115-2406, USA

[c] Department of Computer Sciences, Faculty of Automation and Computer Sciences, Technical University "Politehnica", 1900 Timisoara, ROMANIA

[d] Department of Organic Chemistry, Chemical Engineering Faculty, University "Politehnica", Str. Bocsa 6, 1900 Timisoara, ROMANIA

[e] Chemical Institute of Romanian Academy, Bd. M. Viteazul 24, 1900 Timisoara, ROMANIA

Abstract. The quantitative structure – activity relationships are obtained by the MTD procedure for two series of synthetic retinoids: (a) a long series, with n=38 data, and (b) a short series, with n=18 data. These data refer to inhibitory effects of the keratinization of hamster tracheal organ culture (TOC-assay), induction of ornithine decarboxylase (ODC-assay), and inhibition of tumor promotion (antipapilloma – TPA-assay). The COSMIC and HyperChem molecular modeling packages were used for constructing the hypermolecules based on optimized geometries, computing the energies required to convert optimized structure into planar ones, and superposing the retinoid molecules upon RO 13-7410 molecule.

The results of our QSAR study can be summarized as follows: (i) All receptors for retinoids present two binding sites – ionone ring and polyene chain with its terminal -COOH group – and a general hydrophobic character, but they are able to form hydrogen bonds with polar groups of retinoids; (b) The binding site of TOC-assay receptor has more constrained steric requirements for the ionone cycle whereas the ODC-assay receptor binding site

determine more constraint upon the polyene chain and its free end, carboxylate group; (c) The binding site for ODC-assay receptor seems to resemble with that for induction of tumor promotion, but requires somewhat more constraints on molecular stereochemistry. (d) The optimized receptor maps and correlation equations obtained by the MTD procedure can be used for prediction of new highly active synthetic retinoids, with respect to all three or to only one of the biological activities mentioned above.

INTRODUCTION

Retinoic acid and its derivatives have a wide variety of biological effects, mostly related to growth inhibition and induction and differentiation of cells. Regulation of gene activity seems to be the main process, but regulation of other biological activities suggests a pleiotropic mechanism, with several different receptors for retinoic acid. [1]

Conceptually, the chemoprevention of cancer involves intervention in carcinogenic process by an agent that either will block neoplastic inception or arrest or reverse the progression of transformed cells to frank malignant phenotypes. In practice, the total elimination of exposure to carcinogens is infeasible, and in order to achieve a preventive role, the putative interventional agent must therefore enhance the physiological processes that protect the organism against the growth of preneoplastic and neoplastic cells. Retinoids are prime candidate agents for cancer chemoprevention since they regulate cell proliferation and differentiation, and cancer is associated with abnormal growth and with the loss of differentiation. Several structure – activity studies for retinoic acid derivatives were performed, especially related of attempts to use them as reversors in chemotherapy of some forms of cancer. [2]

Receptors for retinoic acid may differ from one organism to another, even for regulation of the same type of gene and, possibly, there are in the same organism receptors related to different types of cellular response. [3] The response to retinoic acid action and of its derivatives by different organisms and tissues can be modulated also by characteristics of transport to the receptor, metabolic activation and deactivation of these molecules. The experimental study of these receptors and modulating factors is, certainly, very laborious and difficult, but the results of several systematic studies concerning different biological activities in large series of retinoids may offer some interesting information about these receptors and modulating factors. QSARs, especially by the MTD method, [4] reveal steric molecular peculiarities for different types of bioactivity, and can be used hereby to compare the characteristics of receptor sites implied in such activities.

Here, we shall analyze by means of the MTD method the peculiarities of the retinoic receptors for inhibition of keratinization of hamster tracheal organ culture (TOC-assay), [5,6,7] induction of ornithine decarboxylase (ODC-assay) [8] and inhibition of tumor promotion in mouse epidermis (TPA-assay). [8] These activities are interrelated to an appreciable extent. There are some sensible differences in activities of some derivatives obtained by different authors – for example, the TOC-assay data of Newton, Henderson and Sporn. [9] Therefore we have used only the data of Dawson et al. [5,6,7,8] where we found a long series (n=38) of retinoids common in TOC and ODC-assays (Table 1) and a short series (n=18) for inhibition of tumor promotion (Table I).

TABLE 1. TOC-assay, ODC assay and TPA-assay data of retinoids (L_i) used in present QSAR analysis; for structures of L_i, see the Figure 1. #

No	L_i	A_{TOC}	A_{ODC}	A_{TPA}	Nr.	L_i	A_{TOC}	A_{ODC}	A_{TPA}
1	Ret_1	11,7	10,5	9,9	23.	Ret_{23}	9,4	9,2	-
2	Ret_2	11,5	8,7	7,7	24.	Ret_{24}	9,4	8,8	-
3	Ret_3	11,2	10,5	9,3	25.	Ret_{25}	9,4	8,1	-
4	Ret_4	11,0	10,4	8,5	26.	Ret_{26}	9,4	7,8	-
5	Ret_5	11,0	10,2	-	27.	Ret_{27}	9,2	8,2	-
6	Ret_6	10,5	9,0	-	28.	Ret_{28}	9,2	9,4	-
7	Ret_7	10,5	8,0	-	29.	Ret_{29}	9,0	8,5	-
8	Ret_8	10,4*	10,3	10,0	30.	Ret_{30}	9,0*	7,6	6,8
9	Ret_9	10,3	9,3	8,5	31.	Ret_{31}	8,7	7,5	-
10	Ret_{10}	10,1	7,2	-	32.	Ret_{32}	8,5	7,8	-
11	Ret_{11}	10,0	8,4	7,2	33.	Ret_{33}	8,5	8,2	-
12	Ret_{12}	10,0	7,7	7,1	34.	Ret_{34}	8,3	7,8	-
13	Ret_{13}	10,0	8,5	-	35.	Ret_{35}	8,0	7,8	-
14	Ret_{14}	9,7	7,3	-	36.	Ret_{36}	8,0	7,8	-
15	Ret_{15}	9,7	8,4	-	37.	Ret_{37}	7,5	7,8	-
16	Ret_{16}	9,7	8,7	7,4	38.	Ret_{38}	7,5	7,8	-
17	Ret_{17}	9,7	8,5	-	39.	Ret_{39}	10,7	9,4	7,3
18	Ret_{18}	9,7	8,5	-	40.	Ret_{40}	10,7	8,9	7,2
19	Ret_{19}	9,7	8,6	8,5	41.	Ret_{41}	10,3	10,0	9,5
20	Ret_{20}	9,5	9,4	-	42.	Ret_{42}	9,4	7,8	6,5
21	Ret_{21}	9,5	8,6	7,5	43.	Ret_{43}	9,1	8,8	7,1
22	Ret_{22}	9,5	8,1	-	44	Ret_{48}	9,7	7,5	6,8

* Alternative values for A_{TOC}: A (Ret_8) = 10.6; A (Ret_{30}) = 9,4; [5]

The values are presented in decreasing order of TOC biological activity. A_{TOC} = -log ED_{50}, where ED_{50} is L_i molar concentration, M (mol/l), producing 50% inhibition of keratinization of tracheal cells in organ culture.[6,7] A_{ODC} = -log ID_{50}, ID_{50} being L_i molar concentration, M (mol/l), producing 50% inhibition of mouse epidermal ODC induction.[8] A_{TPA} = -log ID_{50}, where ID_{50} is L_i molar concentration, M (mol/l), producing 50% inhibition of tumor promotion by TPA.[8]

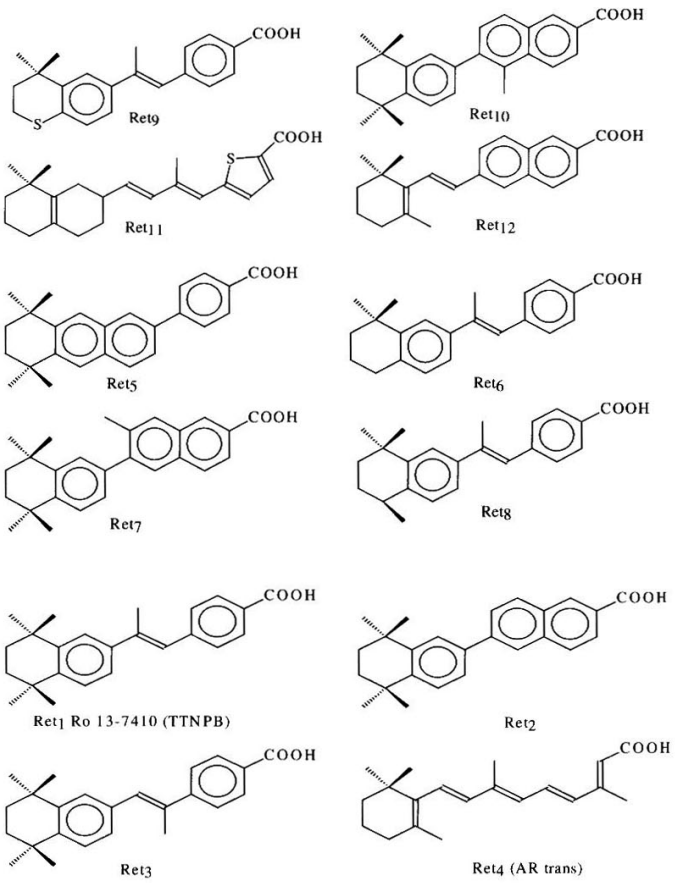

FIGURE 1. Chemical constitutional structures of the retinoids (L_i) used in the QSAR study.

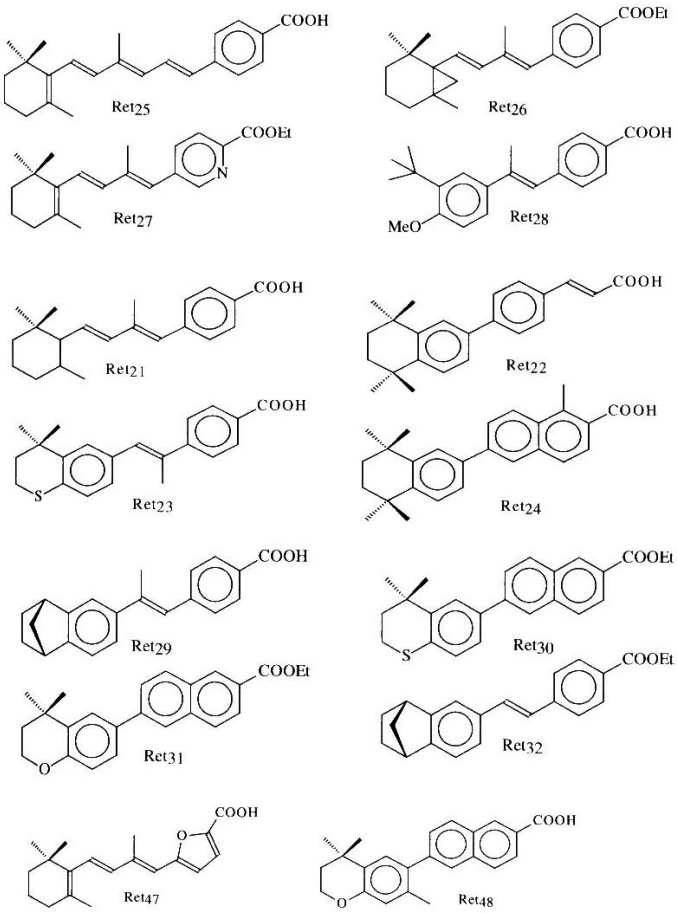

FIGURE 1. (continued)

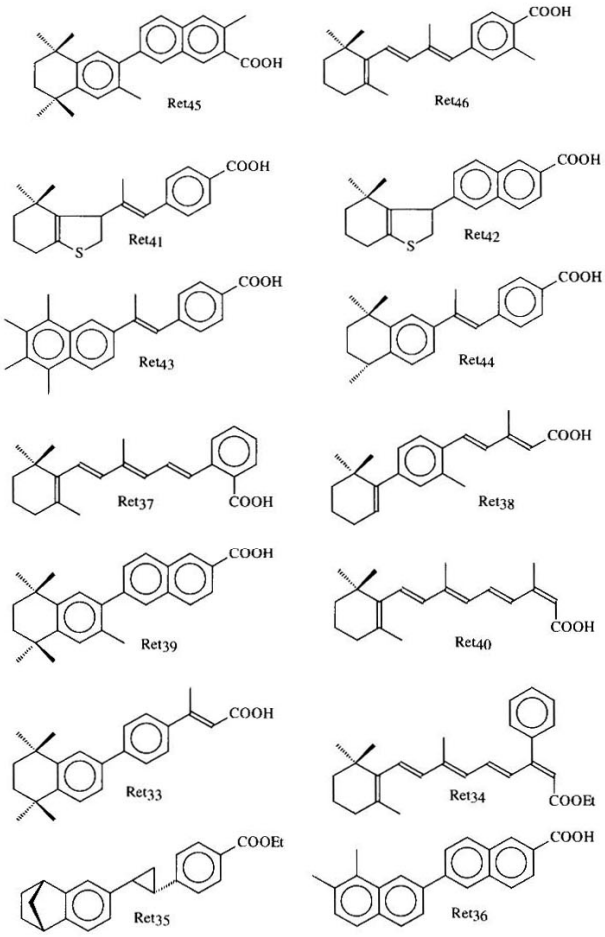

FIGURE 1. (continued)

CORRELATIONS BETWEEN THE THREE TYPES OF ACTIVITY

Linear regression analysis of the ID_{50} values for twenty-two retinoids inhibiting ODC and tumor promotion using 8.5 nmole dose of TPA gave a correlation coefficient r=0.673 ($p<0.001$) and indicates that the ODC assay can be used as a rapid *in vivo* assay to predict the potential ability of retinoids to inhibit tumor promotion. [8]

We recomputed the data of Ref. 5 in order to find out possible inter-correlations between biological activities used in our QSAR study using the MTD method. For a series of 60 compounds we have obtained a linear regression between TOC-assay [5,6,7] and ODC-assay [8] data as follows:

$$A_{TOC} = 4.543(\pm 1.649) + 0.593(\pm 0.194)\, A_{ODC};\ n=60;\ r=0.627;\ s=0.728;\ F=18.4$$

From the above series, we have extracted the 38 compounds for which the linear correlation between the above-mentioned biological activities is:

$$A_{TOC} = 3.403(\pm 2.437) + 0.722(\pm 0.284)\, A_{ODC};\ n=38;\ r=0.647;\ s=0.748;\ F=12.6$$

The last correlation was computed for the large series of retinoids used in this paper.

We find 23 compounds with TOC-assay data [5,6,7] and inhibition of tumor promotion (TPA-assay) data, [8] whereas 24 compounds are common for ODC-assay data [8] and TPA-assay data. [8] The corresponding correlation equations are:

$$A_{TOC} = 7.442(\pm 2.411) + 0.330(\pm 0.296)\, A_{TPA};\ n=23;\ r=0.437;\ s=0.788;\ F=2.4$$
$$A_{ODC} = 3.000(\pm 1.510) + 0.760(\pm 0.185)\, A_{TPA};\ n=24,\ r=0.868;\ s=0.496;\ F=32.2$$

The short series used in this paper has been selected from these two series. The correlation equations A_{TOC}, respectively A_{ODC} *vs.* A_{TPA} are the following:

$$A_{TOC} = 7.000(\pm 2.178) + 0.410(\pm 0.273)\, A_{TPA};\ n=18;\ r=0.602;\ s=0.631;\ F=4.3$$
$$A_{ODC} = 2.740(\pm 1.806) + 0.788(\pm 0.226)\, A_{TPA};\ n=18;\ r=0.868;\ s=0.523;\ F=22.8$$

SURVEY OF PREVIOUS MTD STUDIES

The previous QSAR studies by the MTD method [10,11,12] use TOC-assay as biological activity data [9] and conformationally restricted retinoids, for which the standard geometries are computed. QSAR analysis was separately performed, both for three structural regions (cyclic moiety, polyenic chain, ended functional group) and for the whole molecules. The cyclic moiety corresponds to the atoms C_1-C_8, C_{16}, C_{17} (standard numeration; see Figure 2), and the polyenic chain to the region of atoms C_7-C_{14}, C_{19}, C_{20}, with various shorter or longer chains. The ended functional group corresponds to various functional derivatives of the carboxylic substituent at C_{15} or other structures at this position.

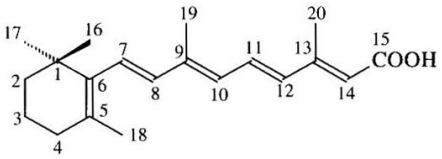

FIGURE 2. The way in which the atoms in retinoic acid are numbered.

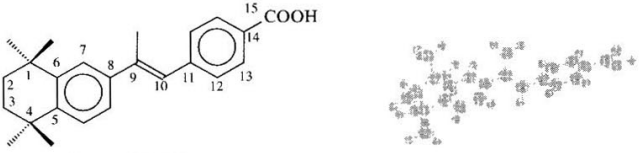

Ret1 Ro 13-7410 (TTNPB)

FIGURE 3. The constitutional structure of RO-7410 (the standard compound for the construction of hypermolecule, **H**) and the corresponding optimized geometry (by MM+ and AM1)

The hypermolecule, **H**, was constructed by atom-by-atom superposition of L_i molecules (for corresponding constitutional structure, see Figure 3) upon the structure of RO 13-7410 as standard, considered the most active ligand in this assay and assuming a restricted

conformation. Due to the fact that "all trans" retinoic acid (see Figure 2) has, according to Newton et al, [9] roughly the same activity (A = -log ED_{50} = 10.52) as the "13-cis" isomer (having the groups 20-CH_3 and 15-COOH of Figure 2 in "Entgegen" orientation), [13] it has been made the assumption that the E-Z isomer transformation in the polyenic chain is a rapid process as compared to those involved in keratinization reversal. Therefore, irrespective of the Z-E type isomers, the compound allowing maximal superposition upon RO 13-7410 molecule (Ret_1 for Table 1 and Figure 1) always has been selected for superposition.

The effect of relative hydrophobicity π, calculated with respect to retinoic acid (π=0) – a strongly hydrophobic molecule (logP = 6.6 for system octanol / water), was rather insignifiant [11] with the series of Newton et al[9] (regression coefficient values being between 0.1 to 0.2), but important in some extent in the series of retinoids with restricted conformation (regression coefficient values being in the domain 0.4 – 0.6). This difference can be explained by the fact that more of the beneficial vertices, (λ= -1), of the hypermolecule **H**, for the second series, are occupied by hydrophobic atoms (or groups of atoms) than in the **H** obtained for the Newton series.

The modifications in the median segment of molecules (polyenic chain) are in agreement with the suggestion that retinoids bind to the receptor by means of two pockets: one for the cyclic moiety, and the second for the carboxylic group. Molecular geometrical studies (using standard geometrical parameters) suggest for the assumed active molecular conformation a distance of 11-14Å between the carbon atoms C_{15} of the carboxylate group and C_6 of the cyclic moiety. As we will see, these results are not in agreement with optimized geometries, obtained by means of MM+ and AM1 methods from HyperChem package. [14] An uninterrupted conjugation in the polyenic chain and an inclusion of aromatic rings with lack of strong steric repulsions in this segment are favorable features, suggesting that rather modest deviations from coplanarity are tolerated in molecules with high activity.

No conclusive QSAR results are available for the end group region. [11,12] Nevertheless, a significant correlation, (r=0.69), with scores of molecules was obtained with an indicator variable, δ_3. For esters, aldehydes, primary alcohols, i.e. functional derivatives easily transformed in –COOH by carboxylate hydrolysis or oxidation, δ_3=1, while for other groups δ_3=0. This suggest that the first class of functional derivatives are primary transformed to carboxylate and, then, possibly, in –COOH, which seems to be important for highly effective molecules.

The long (n = 38) and short (n=18) series of retinoids with ODC and TPA activities are selected from a larger series. [6,7,8] According to comments from Ref. 7, the effects of structural modifications of retinoic acid (RA) skeleton on activity in the ODC- and TPA-assays can be summarized as follows:

(a) Structural modifications were made in the ring, polyolefinic chain and polar-ended region of the retinoic skeleton.

(b) In the polyenic retinoids, as basic RA structure, esters, which would be serve as more lipophilic prodrugs that would be either hydrolyzed or cleaved by esterase to carboxylic acid, were less active than the acids, generally by at least one order of magnitude.

(c) RO 13-7410 (Ret_1 from Figure 1) has 11E-, 13E – cis geometry and an activity comparable with that of "all trans" RA in the ODC-assay but was 25-fold more active at inhibiting tumor promotion. The 9Z – isomer was less active than the 9E – isomer or was inactive. The 13Z – isomer was less active than "all trans" RA but about one order of magnitude. The 7E-, 9E – isomer was less active and the 11E-, 13E – and 9E-, 11E-, 13E – cis configurations enhanced activity in the retinoids.

(d) Polar ended modified retinoids have a decreased activity or they are inactive.

METHOD

In this paper, we used the MTD overlapping technique for QSAR analysis of the retinoids from Table 1. The MTD method, the minimal topological (steric) difference method, allows the description of molecular stereochemistry (of both receptor and ligand molecules, L_i) by indicating the presence or absence of atoms from the considered L_i molecule (i = 1,N) in the vertices of the hypermolecule, **H** (which describes the receptor). The hypermolecule is obtained by an approximately atom-by-atom superposition of the all L_i molecules, neglecting the hydrogen atoms. The hypermolecule **H** can be considered as a topological network in which the vertices correspond to atoms and edges may be viewed as chemical bonds.

During the optimization process, the vertices of **H** are assigned to the receptor cavity, to the receptor walls or to the exterior of cavity, that is the so-called steric irrelevant zone. The

degree of steric misfit for the molecule L_i, i.e., the value of MTD_i, is defined as the sum of the number of cavity vertices of **H** unoccupied by L_i and the number of cavity vertices of **H** occupied by L_i. The whole number of **H** (meaning cavity, wall and irrelevant zone) obtained by the optimization procedure makes up a hypothetical steric receptor map.

The actual improved MTD method takes into consideration the (possible) conformational flexibility of the effectors L_i (considering for each L_i multiple low energy conformations) and the series of drugs with some compounds for which only threshold bioactivities or their intervals are known (if, it is the case). The cross-validation procedure is also used in order to assess the reliability of the obtained results. The molecular mechanics techniques are used in the superposition process for designing the hypermolecule **H**.

H is used as a topological framework for describing the stereochemistry of the drug molecules and of the receptor sites by the vectors $\mathbf{X} = \{x_{ijk}\}$ and $\mathbf{V} = \{v_j\}$, i = 1,2...n; j = 1,2...m; k = 1,2...C_i. The entry x_{ijk} is taken to be 1 if the vertex j of **H** is occupied by a non-hydrogen atom of the molecule i being in conformation k, and $x_{ijk} = 0$ if it is not occupied. The stereochemistry of the receptor site is described by the vector **V**, having as elements a ternary parameter v_j (j = 1,m), associated to each vertex j; $v_j = -1$ should correspond to vertices situated in the cavity of the receptor site, $v_j = +1$ are assigned to the receptor walls, and $v_j = 0$ represent the vertices situated outside of the receptor. Thus, the hypermolecule, which simulates the receptor site in the optimization process, is divided into **m** cells (that can be approximated by the mean values of vdW volumes of the corresponding atoms) by the N molecules M_i, which "investigate" the receptor space. If a molecule M_i has several low energy conformations, it will adopt the one that fits best to the receptor, i.e., that conformation with the lowest MTD value. For a given receptor map represented by the vector **V**, the MTD value for the molecule i, MTD_i, is given by:

$$MTD_{ik} = \left(s + \sum_{j=1}^{m} v_j \cdot x_{ijk} \right); \quad MTD_i = \min_k (MTD_{ik}) \qquad (1)$$

where m and s stand for the number of **H** vertices, and the number of cavity vertices, respectively.

The mapping of receptor space for a given series of ligands, L_i, optimizes [15] the (hypothetical) shape of the biological receptor by using the regression analysis. The

information for the description of the receptor is given as a set of experimental biological activities, A_i, for an N number of molecules M_i. It is supposed that the biological activities are measured in the same conditions for all the M_i compounds, with the same accuracy and precision.

The structure of the receptor map (denoted here by **V**) obtained based on the hypermolecule **H**, which is constructed by atom per atom superposition of all the molecules, M_i, is described by the vector **V**:

The computational procedure implies the evaluation of the steric parameter MTD for each of the M_i molecules with respect to the receptor map **V,** by means of relations (1), with s defined as

$$s = \sum_{j=1}^{m} |v_j|, \quad \text{for all } v_j = -1 \tag{2}$$

The correlation coefficient (r) has been used as the optimization criterion. The fundamental of this method consists in modifying the topography of hypermolecule **H** by moving the cavity vertices to wall and to irrelevant zone, the irrelevant vertices to cavity and wall, and so on, until one obtains the best shape of the analyzed receptor, corresponding to the optimal linear model, as measured by correlation coefficient r. For more details, one may consult Refs. 4 and 15.

RESULTS AND DISCUSSIONS

Construction of the Hypermolecule and Molecular Modeling Calculations

One obtains the hypermolecule **H** by approximate atom per atom superposition of the all (N) molecules (N = 37 for large series, Ret_i, I = 2,38, and N = 17, Ret_i, I = 2, 18, from short series) of the database (Table 1 and Figure 1) upon the standard molecule (S), that is S = RO 13-7410), seeking maximal superposition. The compounds of long series are presented in Table 5, and those of short series in Table 6. Such a superposition procedure is the basis for the description of molecular stereochemistry in the MTD. Actually, this process is performed interactively using the optimized geometries of the ligand molecules, computed with the aid of molecular mechanics force fields or, alternatively, classical 2D chemical formulas. [15]

Efforts to extract three-dimensional information regarding ligand – (unknown) receptor (L–R) interaction from measurements of potency are generally centered on the QSAR domain, and appropriate characterization of the molecular shape is the major obstacle in the development of a topographical basis for QSAR.

The superposition of the N molecules L_i yields a 2D or 3D hypermolecule **H**, in fact a topological (2D or 3D) network. This network consists of **m** vertices, j, corresponding to the approximate position of atoms (in 2D or 3D space) in the superimposed molecules, while the edges can be assimilated to chemical bonds between the atoms. The main purpose of **H** is to reflect the stereochemistry of drug molecules bound to the receptor site.

The previous survey suggests that the receptor responsible for epithelial differentiation requires a conformation of the active retinoic molecules similar to that of the RO 13-7410. This means approximately planar geometry due to the conjugation of the extended π-electronic system. In the MTD studies [10,11,12] already mentioned, the hypermolecule was constructed based upon comparison of Dreiding models. In this approach, the construction of hypermolecule was improved, being performed by the computerized procedure PCFIT from the COSMIC molecular modeling package [16] (for structural manipulation and molecular superposition).

TABLE 2. Distances (in Å) between equivalent atoms resulting by superposition of the cyclic moieties (II, III,...,VI) of Figure 4 upon ionone moiety (I). Structural optimization calculations and superposition were performed by means of the COSMIC computer program. [16]

Superposed cyclic moieties*	Inter-distances between equivalent atoms for pairs of cyclic moieties									
	1-1	2-2	3-3	4-4	5-5	6-6	7-7	8-8	9-9	10-10
II → I	0.02	0.03	0.06	0.10	0.04	0.05	0.02	0.05	0.10	0.08
III → I	0.02	0.07	0.14	0.24	0.22	0.06	0.03	0.05	0.06	0.14
IV → I	0.06	0.28	0.21	0.09	0.07	0.07	0.13	0.19	0.16	0.28
V → I	0.32	0.17	0.12	0.29	0.33	0.20	-	0.56	0.34	0.23
VI → I	0.37	0.10	0.10	0.38	0.97	-	-	-	0.43	0.23
V → VI	0.57	0.11	0.14	0.39	0.72	-	-	-	0.23	0.11

* In superposition of moieties II → I, III → I, IV → I, all 10 pairs of equivalent atom distances were considered for minimization; in superposition procedure of COSMIC V → I, only distances for atoms 1-6, 8-10; in superposition VI → I and V → VI, only for atoms 1-5, 9, 10.

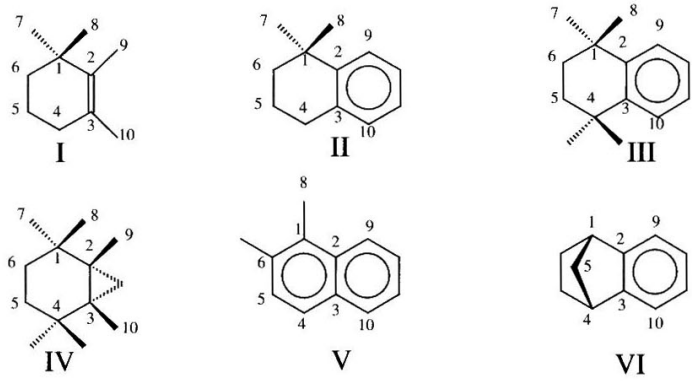

FIGURE 4. Cyclic moieties used for superposition and numeration of equivalent atoms.

The cyclic moieties used for superposition upon the ononic moiety of retinoic acid (structures I – VI) are depicted in Figure 4 and the minimized inter-atomic distances between pairs of equivalent atoms are given in Table 2. With the condition of a maximal 0.5Å inter-distances between atoms which can be considered to occupy the same j-vertex of the hypermolecule, [17] only a single new vertex (j = 17 from atom C_5 of the cyclic moiety VI) had to be introduced with respect to the hypermolecule used in Ref. 11.

Another problem are the steric strain costs for coplanarity in the polyenic chain region, for the retinoids that contain aromatic rings and methyl groups. The structures of interest (VII – XI) are given in Figure 5, and the torsion angles for the minimal energy conformations are listed in Table 3. All computations were performed with the COSMIC package. [16]

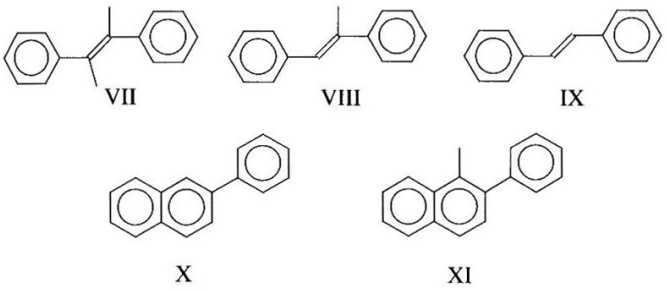

FIGURE 5. Aromatic structures that present steric strain in the polyenic region (C_7-C_{15} of Figure 1).

TABLE 3. Minimal torsion angles and conformational energies (kcal/mole) for aromatic structures with steric strain (see Figure 5 for structures VII – XI) computed with the aid of COSMIC [16] molecular modeling package.

Structure	Θ-r[1)]	Θ-1[2)]	Θ-2[2)]	U_{min}[3)]	U_{plan}[4)]	ΔU[5)]
VII	47.7	64.3	61.1	17.3	120.8	103.5
VIII	1.8	42.6	38.1	14.6	95.8	81.1
IX	0.1	0.0	0.0	10.8	10.8	0.0
X	41.7	-	-	12.5	16.2	3.7
XI	67.1	-	-	15.2	187.1	171.9

[1)] Θ-r : torsion angle between planes of the two aromatic rings in structures VII – XI.
[2)] Θ-1 and Θ-2: angles between the CH_3-C=C- plane (or H-C=C- plane) and the plane of the nearest and furthest aromatic ring, respectively.
[3,4)] U_{min} and U_{plan} are energies (in kcal/mole) for the minimized and the coplanar structure, respectively.
$\Delta U = U_{plan} - U_{min}$ (in kcal/mole)

The structures VII, IX and X are rather planar since the difference in energy, ΔU, required to bring them to co planarity is rather modest. For the structure VII, the methyl group is about 40° out of the plane of the phenyl rings. With 1.5Å for the C-C distance and 120° for the corresponding bond angle, its distance from this plane is of $1.5 \cdot \sin 60° \cdot 2\pi \cdot 40°/360° =$ 0.91Å. The corresponding vertex j = 15 (see Figure 5) could be situated at half way (0.45Å,

i.e. lower than the distance limit of 0.5Å [17]) between the position of a CH_3-group in molecules without steric strain (i.e. planar in the polyenic chain region) and its position in strained molecules (similar to structure VII). The hypermolecules **H**, obtained by superposition of the compounds from Figure 1, corresponding to long series (n=38; see Table 5) and short series (n=18; see and Table 6) are presented in Figures 6 and 7, respectively.

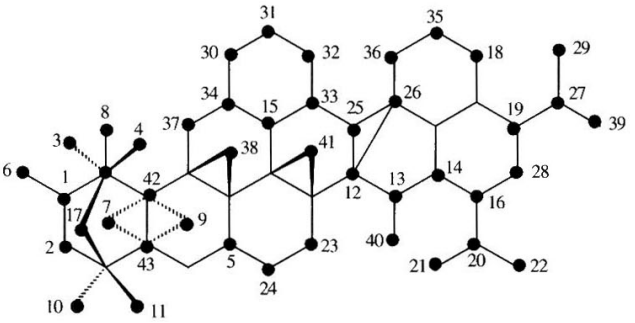

FIGURE 6. The hypermolecule **H** obtained by superposition of compounds from long series (n = 38; see Table 5 and Figure 1).

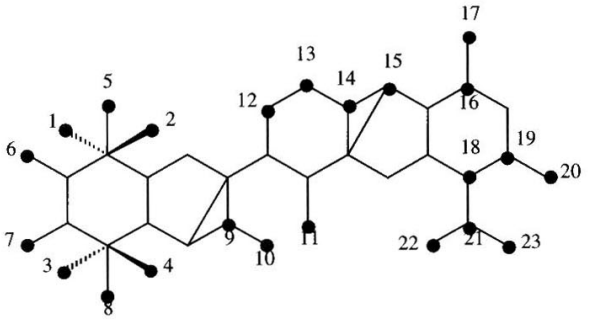

FIGURE 7. The hypermolecule **H** obtained by superposition of compounds from short series (n = 18; see Table 6 and Figure 1).

The construction of hypermolecules corresponding to long (n = 38; Table 5; see Figure 6) and short (n = 18; Table 6; see Figure 7) series have been realized by superposition of the Ret_i , i = 2,43, respectively, Ret_i, i = 2,18 compounds upon Ret_1 (namely RO 13-7410, known as TTNPB), the most active ligand of the studied series. To verify the computed COSMIC results, we have also performed a quantum mechanical calculation for the mentioned studied compounds with the aid of HyperChem computer package. With the purpose of geometry optimization we carry out a MM+ calculation for each molecule (Allinger molecular mechanics force field), followed by an MO AM1 semi-empirical computation. The main geometrical parameters, as resulted from AM1 computations and used in construction of **H**, are presented in Table 4. They were calculated with a RMS gradient less than 0.1 kcal / (Å mol).

TABLE 4. The geometrical parameters for retinoic compounds from Figure 1, calculated with MM+ and AM1 programs (HyperChem package [14]).

No	L_i	d(6-15)	α	φ	No	L_i	d(6-15)	α	φ
1	Ret_1	10,38	104,7	-170,7	23	Ret_{23}	10,16	113,2	82,7
2	Ret_2	10,31	106,6	178,4	24	Ret_{24}	10,35	105,7	-177,8
3	Ret_3	10,16	113,4	83,3	25	Ret_{25}	12,83	134,2	-43,3
4	Ret_4	10,41	98,5	-170,6	26	Ret_{26}	10,12	119,7	149,0
5	Ret_5	10,75	105.7	-168,7	27	Ret_{27}	10,46	107,1	-141,1
6	Ret_6	10,01	121,7	160,5	28	Ret_{28}	8,18	142,4	0,0
7	Ret_7	10,24	106,7	165,2	29	Ret_{29}	10,33	104,6	171,4
8	Ret_8	10,01	122,1	166,1	30	Ret_{30}	10,26	106,9	-166,0
9	Ret_9	10,01	121,4	159,4	31	Ret_{31}	10,31	105,5	-178,1
10	Ret_{10}	10,23	109,6	148,0	32	Ret_{32}	9,97	110,1	-59,6
11	Ret_{11}	9,71	116,4	150,3	33	Ret_{33}	10,00	120,6	175,8
12	Ret_{12}	10,32	127,2	-41,00	34	Ret_{34}	10,61	126,6	-66,7
13	Ret_{13}	10,37	92,9	-80,1	35	Ret_{35}	9,97	110,1	-59,6
14	Ret_{14}	10,37	96,2	-140,5	36	Ret_{36}	10,32	105,3	180.0
15	Ret_{15}	10,12	110,2	-67,9	37	Ret_{37}	9,74	151,6	152,8
16	Ret_{16}	10,21	113,7	-128,2	38	Ret_{38}	10,12	118,7	148,5
17	Ret_{17}	10,25	107,6	166,6	39	Ret_{39}	10,18	111,3	-164,3
18	Ret_{18}	10,14	109,7	-65,7	40	Ret_{40}	10,04	88,5	16,1
19	Ret_{19}	10,01	120,6	160,6	41	Ret_{41}	9,00	142,1	-78,5
20	Ret_{20}	10,26	84,3	83,8	42	Ret_{42}	8,79	132,4	-61,0
21	Ret_{21}	10,07	123,3	118,3	43	Ret_{43}	9,93	129,8	180,0
22	Ret_{22}	10,34	108,3	172,9	44	Ret_{44}	10,38	104,1	-172,6
45	Ret_{45}	9,71	97,0	40,8	46	Ret_{46}	10,13	110,3	62,3
47	Ret_{47}	9,00	120,9	-172,2	48	Ret_{48}	10,17	110,1	165,0

d(6-15) represents the distance between the carbon atoms $C_6 - C_{15}$;
α is the angle between the atoms $C_5 - C_6 - C_{15}$; φ is the dihedral angle $C_5 - C_6 - C_{14} - C_{15}$.

The AM1 results from Table 4 support a topological construction of hypermolecules for two mentioned series, with some nodes in 3D space. Thus, the obtained dihedral angles (φ) for the optimized conformation of Ret_1 (RO 13-7410) are: C_8-C_9-C_{10}-C_{11} = -179,99°; C_8-C_7-C_6-C_1 = -179,47°; C_7-C_6-C_5-C_4 = -179,99. One may observe from these angles that the carbon atoms C_1, C_4 – C_{11} are, actually, in the same plane but the C_2 and C_3 are out of the plane, being about 14.65° below the plane of the other atoms of this molecule.

The distances between the carbon atoms C_{15} of carboxyl (ate) and C_6 of iononic moiety of the compounds of Table 4 are about 10Å, from at least 8.18Å for Ret_{28} to 12.83Å of Ret_{25}. In fact, only ten derivatives of RA have the distance C_{15} – C_6 less than 10Å, namely Ret_{11} (9.71 Å), Ret_{28} (8.18 Å), Ret_{32} (9.97 Å), Ret_{35} (9.97 Å), Ret_{37} (9.74 Å), Ret_{41} (9.00 Å), Ret_{42} (8.79Å), Ret_{43} (9.93 Å), Ret_{45} (9.71 Å), and Ret_{47} (9,00 Å). Six of them have the distance values very close to 10Å (> 9.70Å) and a single compound, Ret_{25} – above mentioned, has the distance greater than 10.75Å (corresponding to Ret_5). The distance C_6 – C_{15} for the standard structure of Ret_1 (RO 13-7410) is 10.38Å. The data summarized in Table 4 allow the supposition that the polyenic chain modulates the biological activity of two sites of interaction – the iononic moiety and the carboxyl group (or its derivatives). The carboxyl ended presents a higher conformational flexibility.

The results obtained by molecular modeling, above described, are in accordance with the hypermolecules from Figures 6 and 7, which approximately depict the stereochemistry of ligand – receptor complexes. The common vertices resulted by superposition have not been numbered because they take a constant contribution to the biological activity. In Table 5 and VI are presented the biological activities and the **X** descriptors for the compounds from long and short series, respectively.

QSAR Analysis by MTD Method

Comparison between TOC and ODC activities was performed considering a series of n=38 molecules (Table 5). For a comparison between TOC, ODC and TPA biological data, only a reduced series of n=18 molecules (Table 6) with experimental values for all three types of bioactivities could be found.

TABLE 5. Structural parameters **X** used in MTD QSAR analysis of long series (n = 38) of retinoic derivatives L_i and the MTD values corresponding to optimized map (S*) of receptor (denoted by MTD*); j indicates the nodes of **H** occupied by the atoms of each L_i.[#]

No	Code	j, x_{ij} = 1 (**X**)	A_{TOC}	MTD*	A_{ODC}	MTD*
1	Ret_1	1 – 5, 10 – 15, 18, 19, 25, 26	11,7	9	10,5	11
2	Ret_2	1 – 5, 10 –15, 18, 19, 25, 26, 33	11,5	10	8,7	12
3	Ret_3	1 – 5, 10 – 14, 18, 19, 23, 25, 26	11,2	10	10,5	11
4	Ret_4	1 – 4, 12 – 16, 18, 19	11,0	10	10,4	11
5	Ret_5	1 – 5, 10 – 14, 18, 19, 23 – 26	11,0	9	10,2	10
6	Ret_6	1 – 5, 12 – 15, 18, 19, 25, 26	10,5	11	9,0	12
7	Ret_7	1 – 5, 10 – 15, 18, 19, 25, 26, 33, 34	10,5	10	8,0	13
8	Ret_8	1 – 5, 11 – 15, 18, 19, 25, 26	10,4	10	10,3	11
9	Ret_9	1 – 5, 12 – 15, 18, 19, 25, 26	10,3	11	9,3	12
10	Ret_{10}	1 – 5, 10 – 15, 18, 19, 23, 25, 26, 33	10,1	10	7,2	12
11	Ret_{11}	1 – 4, 12 – 15, 18, 19, 26	10,0	11	8,4	12
12	Ret_{12}	1 – 4, 12 – 15, 18, 19, 25, 26	10,0	11	7,7	13
13	Ret_{13}	1 – 5, 10 – 14, 18, 19, 25, 26	10,0	10	8,5	11
14	Ret_{14}	1 – 4, 12 – 16, 18, 19, 30 – 34	9,7	11	7,3	14
15	Ret_{15}	1 – 4, 12 – 15, 18, 19, 25, 26	9,7	11	8,4	12
16	Ret_{16}	1 – 4, 12 – 15, 18, 19, 23, 25, 26	9,7	11	8,7	12
17	Ret_{17}	1 – 5, 10 – 16, 18, 19, 25, 26, 33	9,7	10	8,5	12
18	Ret_{18}	1 – 4, 12 – 15, 18, 19, 25, 26, 40	9,7	11	8,5	12
19	Ret_{19}	1 – 5, 12 – 15, 18, 19, 25, 26	9,7	11	8,6	12
20	Ret_{20}	1 – 4, 12 – 15, 18, 19, 25, 26, 38	9,5	11	9,4	11
21	Ret_{21}	1 – 4, 12 – 15, 18, 19, 25, 26	9,5	11	8,6	12
22	Ret_{22}	1 – 5, 10 – 12, 15, 18, 19, 25, 26, 33	9,5	11	8,1	13
23	Ret_{23}	1 – 5, 12 – 14, 18, 19, 23, 25, 26	9,4	12	9,2	12
24	Ret_{24}	1 – 5, 10 – 15, 18, 19, 25, 26, 33, 36	9,4	11	8,8	12
25	Ret_{25}	1 – 4, 12 – 16, 19, 27 – 29, 39	9,4	11	8,1	13
26	Ret_{26}	2, 4, 7 – 9, 12 – 15, 18, 19, 25, 26	9,4	11	7,8	13
27	Ret_{27}	1 – 4, 12 – 15, 18, 19, 25, 26	9,2	11	8,2	12
28	Ret_{28}	1, 3 – 5, 11 – 15, 18, 19, 25, 26	9,2	11	9,4	11
29	Ret_{29}	5, 12 – 15, 17 – 19, 25, 26, 42, 43	9,0	12	8,5	13
30	Ret_{30}	1 – 5, 12 – 15, 18, 19, 25, 26, 33	9,0	12	7,6	13
31	Ret_{31}	1 – 5, 12 – 15, 18, 19, 25, 26, 33	8,7	12	7,5	13
32	Ret_{32}	5, 12 – 14, 17 – 19, 25, 26, 42, 43	8,5	13	7,8	13
33	Ret_{33}	1 – 5, 10 – 12, 15, 18, 19, 25, 26, 33, 36	8,5	12	8,2	13
34	Ret_{34}	1 – 4, 12 – 16, 18, 20 – 22, 26, 35, 36	8,3	13	7,8	13
35	Ret_{35}	5, 12 – 14, 17 – 19, 25, 26, 41 – 43	8,0	13	7,8	13
36	Ret_{36}	1, 2, 5, 6, 8, 12 – 15, 18, 19, 25, 26, 33	8,0	13	7,8	13
37	Ret_{37}	1 – 4, 12 – 16, 19, 20 – 22, 28	7,5	14	7,8	13
38	Ret_{38}	1 – 4, 15, 18, 19, 25, 26, 33, 34, 36, 37	7,5	14	7,8	13

[#] The biological activities A_{TOC} and A_{ODC} correspond, respectively, to TOC-assay and ODC-assay.

TABLE 6. Structural parameters **X** used in MTD QSAR analysis of short series (n = 18) of retinoic derivatives L_i and the MTD values corresponding to optimized map (S*) of receptor (denoted by MTD*); j indicates the nodes of **H** occupied by the atoms of each L_i.[#]

No	Code	j, x_{ij} = 1 (**X**)	A_{ICTH}	MTD*	A_{IODC}	MTD*	A_{ITES}	MTD*
1	Ret_1	1 – 4, 9, 12, 14 – 17	11,7	4	10,5	4	9,9	3
2.	Ret_2	1 – 4, 9, 12 – 17	11,5	4	8,7	5	7,7	4
3	Ret_3	1 – 4, 9, 11, 14 – 17	11,2	4	10,5	4	9,3	3
4	Ret_4	1, 2, 12, 18 – 20	11,0	5	10,4	4	8,5	4
5	Ret_{39}	1 – 4, 9, 10, 12 – 17	10,7	5	9,4	5	7,3	5
6	Ret_{40}	1, 2, 12, 18, 21 – 23	10,7	5	8,9	5	7,2	5
7	Ret_8	1, 2, 4, 9, 12, 14 – 17	10,6	5	10,3	4	10,0	3
8	Ret_{41}	1, 2, 12, 14 – 17	10,3	6	10,0	5	9,5	4
9	Ret_9	1, 2, 9, 12, 14 – 17	10,3	6	9,3	5	8,5	4
10	Ret_{11}	1, 2, 12, 15 – 17	10,0	6	8,4	6	7,2	5
11	Ret_{12}	1, 2, 12 – 17	10,0	6	7,7	6	7,1	5
12	Ret_{19}	1, 2, 9, 12, 14 – 17	9,7	6	8,6	5	8,5	4
13	Ret_{16}	1, 2, 11, 12, 14 – 17	9,7	6	8,7	5	7,4	5
14	Ret_{48}	1, 2, 9, 12 – 17	9,7	6	7,5	6	6,8	5
15	Ret_{21}	1, 2, 12, 14 – 17	9,5	6	8,6	5	7,5	4
16	Ret_{42}	1, 2, 12 – 17	9,4	6	7,8	6	6,5	5
17	Ret_{30}	1, 2, 9, 12 – 17	9,4	6	7,6	6	6,8	5
18	Ret_{43}	5 – 9, 12, 14 – 17	9,1	7	8,8	5	7,1	5

[#] The biological activities A_{TOC}, A_{ODC} and A_{TPA} correspond, respectively, to TOC-assay, ODC-assay and TPA-assay.

The long series of n = 38 molecules L_i (I = 1,38) are extracted from a series of n = 42 molecular structures, selected such as to allow a maximal superposition upon the Ret_1 (RO 13-7410). The L_i have a free –COOH group or a simple methyl or ethyl ester group. Four molecules, Ret_{44} – Ret_{47} (see Table 1, and Figure 1 for structures), were eliminated because they gave, in preliminary MTD studies, large differences between experimental (*A*) and calculated (**A**) values for both TOC and ODC activities. While for Ret_{46} and Ret_{44}, the presence of a methyl group in ortho to the carboxyl group (which can produces an out of plane of the –COOH group) could explain the *A* – **A** differences, there is no plausible explanation for the other two eliminated molecules.

The optimized maps of receptor, S*, resulted by optimization procedure for the molecules of Table 5 and Table 6, and vertex attributions to receptor cavity (v_j = -1), receptor walls (v_j = +1) and exterior regions (v_j = 0), are depicted in Figure 8 for TOC- and ODC-activities (long series), and in Figure 9 for TOC-, ODC-, and TPA-activities (short series). The molecular structures of retinoic ligands, L_i, are showed in Figure 1.

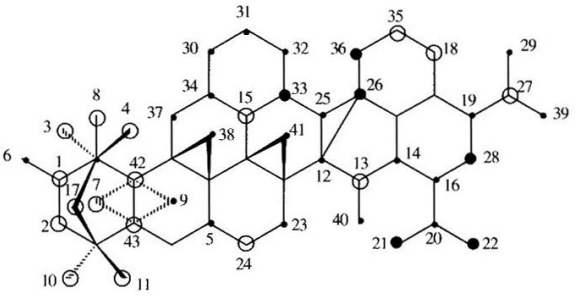

FIGURE 8. The optimized receptor maps S^*_{TOC} and S^*_{ODC} for long series of retinoids (n = 38) in TOC- and ODC-assays; cavity vertices (v_j = -1): open circles; wall vertices (v_j = +1): full circles; exterior vertices (v_j = 0): dots.

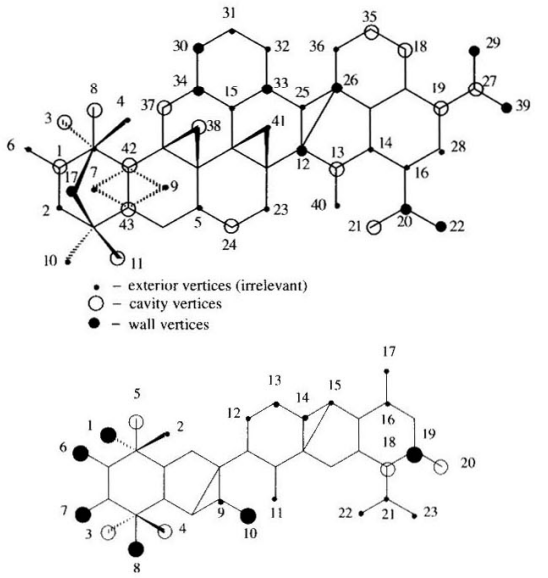

FIGURE 9. The optimized receptor maps S^*_{TOC}, S^*_{ODC} and S^*_{TPA} for short series of retinoids (n = 18) in TOC-, ODC- and TPA-assays; cavity vertices (v_j = -1): open circles; wall vertices (v_j = +1): full circles; exterior vertices (v_j = 0): dots.

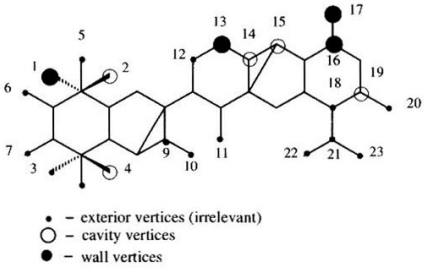

FIGURE 9. (continued)

Recall that MTD_i value is a measure of steric misfit of molecule L_i within the receptor map and is equal to the number of unoccupied cavity vertices plus occupied wall vertices – see relations (1) and (2), with k = 1 (one single conformation for each L_i).

The real predictive power of our QSAR results was tested by a cross-validation like procedure. The molecules, previously arranged in the decreasing order of activity for each biological assay, were separated in a EVEN (I = 1, 3, 5, ...) and ODD (I = 2, 4, 6, ...) subseries. Afterwards, the receptor maps were again optimized and the corresponding correlation equation for each subseries was in turn used to calculate activities for the other ("test") series. Correlation between experimental and calculated activities for entire series yields the cross-validation coefficient, r^2_{CV}.

The optimized receptor maps, S* (see Figure 8), correlation equations and MTD cross-validation results from long series are the following:

$$S^*_{TOC} \begin{cases} j(\lambda_j = -1)\text{: } 1-4, 7, 8, 10, 11, 13, 15, 17, 18, 24, 27, 35, 42, 43 \\ j(\lambda_j = 0)\text{: } 5, 6, 9, 12, 14, 16, 19, 20, 23, 25, 29, 30-32, 34, 37-41 \\ j(\lambda_j = +1)\text{: } 21, 22, 26, 28, 33, 36 \end{cases}$$

$$\hat{A}_{ICTH} = 18{,}246(\pm 1{,}254) - 0{,}775(\pm 0{,}112)MTD \qquad (3)$$

$$n = 38;\ r = 0{,}920;\ s = 0{,}403;\ F = 96{,}8;\ r^2_{CV} = 0{,}800$$

$$S^*_{ODC} \begin{cases} j(\lambda_j = -1)\text{: } 1, 3, 8, 11, 13, 18, 19, 21, 24, 27, 35, 37, 38, 42, 43 \\ j(\lambda_j = 0)\text{: } 2, 4-7, 9, 10, 14-16, 23, 25, 28, 31, 32, 36, 40, 41 \\ j(\lambda_j = +1)\text{: } 12, 17, 20, 22, 26, 29, 30, 33, 34, 39 \end{cases}$$

$$\hat{A}_{IODC} = 19{,}125(\pm 2{,}450) - 0{,}868(\pm 0{,}201)MTD \quad (4)$$

n = 38; r = 0,826; s = 0, 520; F = 37,5; $r^2_{CV} = 0{,}682$

The correlation equations *A vs.* MTD, the optimized receptor maps, S* (see Figure 9), and MTD cross-validation results from short series are the following:

$$S^*_{TOC} \begin{cases} j(\lambda_j = -1)\text{: } 3-5, 18, 20 \\ j(\lambda_j = 0)\text{: } 2, 9, 11-17, 21, 23 \\ j(\lambda_j = +1)\text{: } 1, 6-8, 10, 19 \end{cases}$$

$$\hat{A}_{ICTH} = 14{,}864(\pm 0{,}926) - 0{,}840(\pm 0{,}166)MTD \quad (5)$$

n = 18; r = 0,930; s = 0,294; F = 47,8; $r^2_{CV} = 0{,}853$

$$S^*_{ODC} \begin{cases} j(\lambda_j = -1)\text{: } 2, 4, 14, 15, 19 \\ j(\lambda_j = 0)\text{: } 3, 5-12, 18, 20-23 \\ j(\lambda_j = +1)\text{: } 1, 13, 16, 17 \end{cases}$$

$$\hat{A}_{IODC} 15{,}587(\pm 1{,}318) - 1{,}306(\pm 0{,}285MTD) \quad (6)$$

n = 18; r = 0,930; s = 0,386; F = 48,0; $r^2_{CV} = 0{,}745$

$$S^*_{TPA} \begin{cases} j(\lambda_j = -1)\text{: } 4, 14, 19 \\ j(\lambda_j = 0)\text{: } 2, 3, 5, 6, 9, 15-18, 20-23 \\ j(\lambda_j = +1)\text{: } 1, 7, 8, 10-13 \end{cases}$$

$$\hat{A}_{ITES} = 13{,}740(\pm 1{,}298) - 1{,}340(0{,}295)MTD \quad (7)$$

n = 18; r = 0,915; s = 0,467; F = 38,7; $r^2_{CV} = 0{,}781$

One may observe from the above correlation equation that we have obtained good statistical results, the correlation coefficients being r > 0.900, with one exception – the equation (4) in which r = 0.826 and $r^2_{CV} = 0.682$. For long series and ODC-assay, the MTD steric indicator explains only 68% from variance of predicted activities by Eq.

(4). Thus, within this series of molecules with high hydrophobicity and a distance of approximately 10Å between C_{15} of –COOH group and C_6 of iononic moiety, it is important to introduce other structural parameters able to quantify the hydrophobic molecular structural characteristics.

Comparison of TOC and ODC results for long series, i.e., the optimized maps S^*_{TOC} and S^*_{ODC}, indicates a bulkier region in the iononic cycle zone of TOC receptor, accommodating the greater cycles, than for the ODC receptor. In this last case, most steric constraints in the polyenic chain and terminal –COOH region are required (see Figure 8).

For the short series (n=18), with compounds that present all three types of activity, the hypermolecules contains a smaller number of non-common numbered vertices. There are some differences in the attribution of cavity, wall and exterior vertices for the three optimized receptor maps, S^*_K, k = *TOC, ODC, and TPA*.

On the basis of optimized maps and Equations (3) – (7) we propose new structures with higher activity, with respect to all three or to only one of the studied activities (see Figure 10).

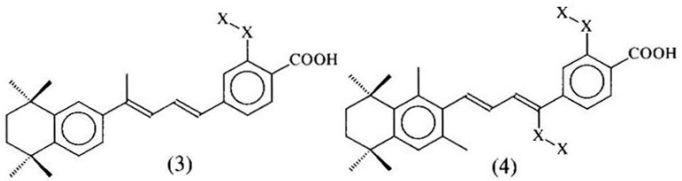

(3) (4)

ATOC=13.6 AODC=13.0

FIGURE 10. Proposal of new chemical structures with increased activities. The predicted activities are listed below each structural formula, as calculated with Equations (3) and (4).

CONCLUSIONS

According to the optimized receptor maps and intercorrelation coefficients obtained for all three types of biological activity data, two aspects related to general structural requirements of retinoid receptor and, also, to similitude and differences between these types of receptors, can be summarized as follows:

1. All receptors for retinoids possess at least two binding sites. One site accommodates the iononic ring and the other should partly bind the polyenic chain and the negatively charged carboxyl group. At these requirements, one must add a predominant general hydrophobic character and the possibility to form hydrogen bonds with hydrophilic groups in different positions of the retinoid molecules (if available).
2. The binding site of each receptor for retinoids (corresponding to three types of processed biological activities) presents some differences from one to another, and these can be resumed like that.

TOC-Assay Receptor vs. ODC-Assay Receptor (Long and Short Series)

The binding site for the iononic cycle presents for the TOC-assay receptor a more spatially extended attractive region in comparison with the ODC-assay receptor, where the steric strain is less stringent. At the level of the second binding site, for the ODC-assay, there is an about equal increase in number of both cavity and wall vertices (comparatively with TOC-assay receptor) and the global effect is, approximately, the same for both receptors. Therefore, we can assume that, at this level, the retinoids are more sterically constrained by the ODC-assay receptor than by the TOC-assay receptor.

ODC-Assay Receptor vs. TPA-Assay Receptor (Short Series)

According to the optimized receptor maps and to good correlation coefficient between ODC-assay and tumor promotion data (r=0.868), both retinoid receptor binding sites present the same structural characteristics and the level of steric constrains for retinoid molecules.

This steric constrains are increased at the second binding site and decreased at the first binding site comparatively with TOC-assay receptor. Therefore, the binding site for the TPA-receptor should have more extended wall regions than the ODC—assay receptor and the steric conformational constrains are increased.

All these conclusions are in rather good agreement with those of Dawson et al [9] but produce some supplementary stereochemical information. The quantitative treatment of this retinoids provides proposals for new synthetic retinoid structures with high activity for one or all three types of biological activity (see Figure 10).

ACKNOWLEDGEMENT

The authors wish to express their gratitude to Dr. J. G. Vinter for COSMIC molecular modeling packages.

REFERENCES

[1] Sherman, M. I., (Ed.), *Retinoids and Cell Differentiation,* CRC Press, Boca Raton, Fl, 1986.

[2] Dawson, M. I. And Okamura, W. H., (Eds.), *Chemistry and Biology of Synthetic Retinoids*, CRC Press, Boca Raton, Fl, 1990.

[3] Sporn, M. B., Roberts, A. B., Goodman, D. S., *The Retinoids. Biology, Chemistry, and Medicine,* Raven Press, New York, 1994.

[4] Simon, Z., Chiriac, A., Holban, S., Ciubotariu, D., Mihalas, I., *Minimum Steric Difference. The MTD Method for QSAR Studies,* Wiley (Res. Stud. Press, Letchworth), New York, 1984.

[5] Schiff, L. J., Okamura, W. H., Dawson, M. I. and Hobbs, P. D., Structure – biological activity relationships of new synthetic retinoids on epithelial differentiation of cultured hamster trachea, in Dawson, M. I., Okamura, W. H. (Eds.) *Chemistry and Biology of Synthetic Retinoids*, CRC Press, Boca Raton, Fl, 1990, pp. 307 – 364.

[6] Dawson, M. J., Hobbs, P. D., Derdzinski, K., Chan, R. L., Gruber, J., Chao, W., Smith, S., Thies, R. W., Schiff, L. J., Conformationally restricted retinoids, *J. Med. Chem.*, **1984**, *27*, 1516 – 1523.

[7] Dawson, M. J., Hobbs, P. D., Chan, R. L., Chao, W., Fung, V. A., Aromatic Retinoic Acid Analogues. Synthesis and Pharmacological Activity, *J. Med. Chem.*, **1981**, *24*, 583 – 592.

[8] Dawson, M. I., Chao, W., Hobbs, P. D. and Delair, T, The inhibitory effects of retinoids on the induction of ornithine decarboxylase and the promotion of tumors in mouse epidermis, in Dawson, M. I., Okamura, W. H. (Eds.) *Chemistry and Biology of Synthetic Retinoids*, CRC Press, Boca Raton, Fl, 1990, pp. 385 – 466.

[9] Newton, D. L., Henderson, W. R., Sporn, M. B., Structure – activity relationships in hamster tracheal organ culture, *Cancer Res.*, **1980**, *40*, 3413 – 4323.

[10] Niculescu – Duvăz, I., Ionescu, A., Voiculetz, N., Simon, Z., Relations quantitatives structure – activité appliqués à deux classes d'inhibiteurs de la carcinogènes chimique, *Rev. Roum. Morphol. Embriol. Physiol*, **1985**, *22*, 135 – 143.

[11] Niculescu – Duvăz, I., Simon, Z., Voiculetz, N., QSAR Application in Chemical Carcinogenesis. I. QSAR Analysis of a class of carcinogenesis inhibitor : retinoids, *Carcinogenesis*, **1985**, *6*, 479 – 486.

[12] Niculescu – Duvăz, I., Simon, Z. , Voiculetz, N., Carcinogenesis inhibitory properties of retinoids: a QSAR – MTD analysis, in Dawson, M. G., Okamura, W. H., *Chemistry and Biology of Synthetic Retinoids*, CRC Press, Boca Raton, Fl, pp. 575 – 606.

[13] Gergen, J., Bohl, M., Simon, H., and Simon, Z., Structure activity relations for steroids by the MTD method. Superposition procedure for molecules with different condensed cycles, *Rev. Roum. Chim.*, **1989**, *34*, 995 – 1005.

[14] We thank to Dr. M. Mracec for HyperChem computations.

[15] Ciubotariu, D., Medeleanu, M., Gogonea, V., The van der Waals Molecular Descriptors and the New Variant of the MTD Method, in Diudea, M. V. (Ed.), *Molecular Descriptors for QSPR/QSAR Studies,* Nova Science, USA, 2000, Chapter 11.

[16] Morley, S. D., Abraham, R. J., Haworth, I. S., Jackson, D. E., Saunders, M. R., and Vinter, J. G. COSMIC (90): An improved molecular mechanics treatment of hydrocarbons and conjugated systems, *J. Comput. Aid. Mol. Des.* **1991**, *5*, 475 – 504.

[17] Oprea, T. I., Ciubotariu, D., Sulea, T. and Simon, Z., Comparison of the Minimal Steric Difference (MTD) and Comparative Molecular Field Analysis (CoMFA) Methods of Binding of Steroids to Carrier Proteins, *Quant. Struct.-Act. Relat.* **1993**, *12*, 21 – 26.